ELSEVIER

Contents lists available at ScienceDirect

# Colloids and Surfaces A: Physicochemical and Engineering Aspects

journal homepage: www.elsevier.com/locate/colsurfa





# Adsorption of chalcophile metals onto thiol-based resins: Modeling adsorption capacity and behavior using surface complexation modeling

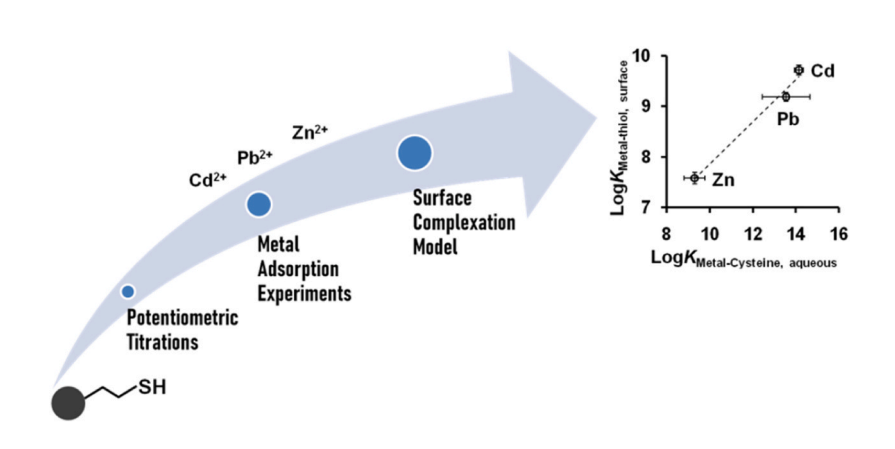
Qiang Yu\*, Jeremy B. Fein

Department of Civil & Environmental Engineering & Earth Sciences, University of Notre Dame, Notre Dame, IN 46556, United States

#### HIGHLIGHTS

- Cd adsorption onto thiol-based resins is controlled by proton-active thiol sites.
- Surface complexation modeling accounts for Zn, Cd, and Pb adsorption on the resins.
- Linear free energy relationships predict stability constants for surface complexes.

#### GRAPHICAL ABSTRACT



### ARTICLE INFO

Keywords:
Adsorption
Chalcophile metal
Thiol
Resin
Surface complexation modeling

### ABSTRACT

Adsorption of chalcophile metals from aqueous solution by thiol resins represents an efficient means of reusing these metals and remediating waste streams, and a predictive modeling approach is needed in order to design and optimize adsorption applications. In this study, potentiometric titration measurements, metal adsorption experiments and surface complexation modeling (SCM) approaches were used to characterize three thiol-based resins (BT40, SP70, and SP300), and to model their proton, Cd, Zn, and Pb adsorption capacities and behaviors. We find that the extent of Cd adsorption onto the three resins correlates strongly to the measured concentration of proton-active thiol sites on each resin, and that the BT40 resin has a significantly higher concentration of proton-active thiol sites than the other two resins tested. Using the BT40 as a model resin, we demonstrate that the measured stability constant (*K*) of the Cd-thiol surface complex on the resin successfully accounts for the effects of both the metal:resin ratio and pH over a wide range of experimental conditions. We also find that a linear free-energy relationship (LFER) exists between the *K* values of metal-thiol surface complexes on the BT40 resin and the *K* values of metal-thiol aqueous complexes for Cd, Zn and Pb. This LFER can be used to estimate the *K* values of other metal-thiol resin surface complexes that have not been measured experimentally, therefore enabling prediction of the adsorption behavior of a wide range of metals onto thiol-based resins under a wide range of system conditions. This study demonstrates that a SCM approach, coupled with potentiometric titration

<sup>\*</sup> Corresponding author.

E-mail address: qyu@nd.edu (Q. Yu).

measurements and metal adsorption experiments, represents a powerful tool for the design and optimization of strategies for separating and recovering chalcophile metals from aqueous media.

#### 1. Introduction

Chalcophile metals, such as Hg, Cd, Pb, Au, Pd and Ag, are a class of metals that bond more readily with sulfur than with oxygen. Many chalcophile metals are of environmental and/or industrial significance [1,2]. For example, Hg, Cd and Pb are highly toxic and their presence in surface and ground water is of continuous environmental concern. Au, Pd and Ag, on the other hand, are precious metals that have low natural abundance and are increasingly used in industrial fields such as electronics, catalysis and medicine. Much effort has been made over the past few decades to develop efficient strategies for removing and recovering chalcophile metals from aqueous media in order to move toward sustainable use of precious metals and to diminish the discharge of toxic metals to the environment [2–6]. Because metals do not decompose, physical separation approaches such as adsorption represent the most promising technologies for not only the recovery but also the removal of chalcophile metals from aqueous media.

Due to the strong interactions between sulfur and chalcophile metals, many studies have focused on developing thiol-based resins for the separation of chalcophile metals from solution [7-12], and currently a range of thiol-based resin types are commercially available. Thiol-based resins exhibit not only high adsorption capacities but also excellent selectivity for chalcophile metals [7,11]. In general, the concentration of thiol sites on a resin surface controls the adsorption capacity of the resin. However in practice, the concentration of a metal that adsorbs onto a resin under a specific set of conditions is also affected by a range of other resin properties (e.g., bead size, porosity, the configuration and type of thiol sites on the surface) and water chemistry factors (e.g., pH, the concentration of competing cations, the concentration of ligands that form aqueous complexes with the metals, etc.) [10,11,13]. In previous studies of metal adsorption onto thiol-based resins, empirical models such as Langmuir or Freundlich isotherm approaches have been used to describe the adsorption behavior [12–14]. Because these models are not mechanistic, they should be applied only to the specific conditions that were used for the adsorption experiments, and should not be extended to other conditions that were not tested [15,16]. Although the maximum monolayer adsorption capacity  $(q_e)$  from Langmuir isotherm models has been used as an indicator of adsorption capacity of a sorbent in previous studies [12–14], the value of  $q_e$  from an experimental study depends directly on the experimental conditions. Therefore, a direct comparison of experimentally determined  $q_e$  values from adsorption experiments that were conducted under different solution conditions does not provide useful information, and this also explains why reported  $q_e$  values for a metal-sorbent combination can vary by orders of magnitude between experimental studies [12,17]. A more flexible and accurate predictive modeling approach is needed in order to account for the range of parameters that can affect metal adsorption behaviors and to predict adsorption behaviors of metals that have not been studied experimentally.

Surface complexation models (SCMs) are chemical equilibrium models that describe surface complexation reactions that occur on a liquid/solid interface [18]. Similar to the formation of aqueous

complexes, the extent of formation of surface complexes can be described by a complexation reaction and can be quantified with a thermodynamic stability constant (*K*) for the surface complex. SCMs can be used for modeling metal adsorption onto a wide range of materials, such as minerals, bacterial cells, ion exchange resins, biochars, activated carbon and carbon nanotubes [19–27]. Unlike the underlying models in empirical approaches, SCMs are mechanistically accurate, and hence the stability constants for surface complexation reactions do not change as a function of system conditions (other than temperature and pressure). Recently, Mosai et al. used SCM to account for the adsorption of Pd(II) onto a yeast functionalized zeolite as a function of pH, adsorbent dosage, initial Pd concentration and competing ion concentrations [28]. Despite the capabilities of SCMs, metal adsorption behavior onto thiol-based resins has been modeled exclusively using empirical models.

The objective of this study is to test the surface complexation modeling approach to account for and predict the extent of adsorption of chalcophile metals onto thiol-based resins. Our results demonstrate that the measured stability constant of the metal-thiol surface complex on the resin under one metal:resin ratio condition yields accurate predictions of the extent of adsorption of Cd onto the resin under a wide range of pH and metal:resin ratio conditions. We also find that a linear free-energy relationship (LFER) exists between the K values of metal-sulfhydryl surface complexes on the resin and the K values of metal-sulfhydryl aqueous complexes for Cd, Zn and Pb. This LFER can be used to estimate the K values of other metal-sulfhydryl complexes that have not been measured experimentally, thereby enabling prediction of the adsorption behavior of a wide range of metals onto thiol-based resins under a wide range of system conditions.

## 2. Materials and methods

# 2.1. Resins

Three thiol-based resins were used in this study: BT40, SP70 and SP300; and their manufacturers and properties are shown in Table 1. The resins consist of either silica or polystyrene beads treated to be coated with thiol functional groups exclusively. Each of the resins was used as received.

## 2.2. Potentiometric titrations

Potentiometric titrations of suspensions of each type of resin bead and a blank titration of 0.01 M NaCl were conducted using a T7 autotitrator from Mettler Toledo, Inc. and using 1 M HCl or NaOH standards purchased from Fluka Chemical Corp. Prior to each titration, the 0.01 M NaCl solution in which the titration was to be conducted was purged with  $\rm N_2$  for at least 1 h in order to remove dissolved CO2. 100 mg of resin beads were then suspended in 10 mL of the degassed 0.01 M NaCl solution. All of the titrations were conducted in a closed vessel under a  $\rm N_2$  headspace, and each suspension was stirred continuously with a magnetic stir bar. For each titration, two steps were conducted: 1) acidifying the bacterial suspension from the original pH down to pH 3.0 by adding

Table 1
Properties of Thiol-based Resins (manufacturer's data).

Resin	Manufacturer	Size (µm)	Matrix	Functional Group	Thiols (mmol/g)
BT40	Biotage	40–60	Silica	Propanethiol	1.3
SP70	Supra Sciences	70–150	Polystyrene	Thiophenol	2.4-2.5
SP300	Supra Sciences	300–1200	Polystyrene	Thiophenol	4.8–5.0

HCl standard; and 2) a forward titration from pH 3.0 to pH 9.7 by adding NaOH standard. Only these forward titration data were used for the surface complexation modeling to calculate the total sulfhydryl site concentrations. The titrator was set to operate using a method in which the equilibration time for each step of the titration was controlled, and the volume of acid or base added at each step and the associated change in pH were recorded, with a minimum addition volume of 0.25 µL. New titrant was added after the signal drift reached a minimum stability of 0.01 mV/s, or after a maximum waiting time of 60 s. In preliminary experiments, we conducted down-pH titrations from pH 9.7 to pH 3.0 immediately following the forward titrations, and the obtained titration curves (not shown) matched well with their corresponding forward titrations, suggesting rapid reversibility of the protonation reactions and that no significant damage or change occurred to the resin beads during the forward titrations. Triplicate titrations with identical experimental conditions were conducted with the BT40 resin.

In order to compare titration results from different experiments, the results were plotted in terms of the net concentration of protons added to the system:

$$[H^{+}]_{\text{net added}} = C_{\text{a}} - C_{\text{b}} \tag{1}$$

where  $C_a$  and  $C_b$  are the total concentrations of acid and base added to the system during the titration, respectively, with units of mmol/L.

# 2.3. Adsorption experiments

Two sets of adsorption experiments were conducted at ambient conditions. The metal solutions used for the adsorption experiments were diluted from 1000 mg/L (metal concentration) Cd(NO<sub>3</sub>)<sub>2</sub>, Zn (NO<sub>3</sub>)<sub>2</sub> or Pb(NO<sub>3</sub>)<sub>2</sub> commercially-purchased standard solutions using 0.01 M NaCl to the desired concentrations, and all of the solutions were adjusted to pH  $\sim$ 6.0 using 0.1 M NaOH before the experiments.

The first set of adsorption experiments measured the adsorption of Cd onto the BT40, SP70 and SP300 resins (separately) as a function of time. The experimental suspensions were placed in 250 mL Teflon bottles, each of which contained 100 mL of a 0.01 M NaCl solution with 10 mg/L of Cd and 1 g/L of one type of resin, and were rotated end-overend at 60 rpm for 24 h. At 0.5 h, 1 h, 2 h, 3 h, 6 h and 24 h, approximately 2 mL of suspension was removed from each bottle, the sample was filtered using a 0.45  $\mu m$  membrane, and the filtered solutions were analyzed using inductively coupled plasma optical emission spectroscopy (ICP-OES) to determine the concentration of dissolved metal. The extent of adsorption was calculated as the difference between the known initial metal concentration and the measured final metal concentration in solution.

The second set of adsorption experiments measured the adsorption of Cd, Zn and Pb (separately) onto the BT40 resin only, as a function of pH and metal:resin ratio (referred to as metal:resin ratio). In this set of experiments, 30 mL polypropylene test tubes were used as reaction vessels and they were placed on a rotating plate at 60 rpm for 2 h. Each test tube contained 20 mL of a 0.01 M NaCl solution with the desired concentrations of metal and resin beads. Because 10 mg/L of Cd was completely removed by 1 g/L of the BT40 resin in the first set of adsorption experiments, we increased the initial Cd concentration to 50 mg/L in this set of experiments. In order to match the Cd concentration in mol/L, the initial Zn and Pb concentrations were set to 29.5 mg/L and 93.2 mg/L, respectively. Different metal:resin ratios were achieved by varying the resin concentrations from 0.5 to 2.0 g/L. The initial pH values of the systems were adjusted using 0.1 M NaOH or 0.1 M HNO3 in order to achieve pH values within the range of 3.0-7.0. After 2 h of equilibration for each system, the final pH was measured. In this study, all the reported pH values are these final pH readings. The samples were then filtered using a 0.45 µm membrane, and the filtered solutions were analyzed using ICP-OES to determine the concentration of dissolved metal.

#### 2.4. Analysis of metals

A Perkin Elmer Optima 8000 ICP-OES system was used to analyze the concentrations of metals in solution. Matrix-matched standards were prepared by diluting 1000 mg/L commercial standards with 0.01 M NaCl to cover a range of 0.05–5 mg/L for each metal. Prior to analysis, all of the samples were diluted to the concentration ranges covered by the standards using 0.01 M NaCl. 1000  $\mu g/L$  of yttrium was added to each sample and was measured at a wavelength of 371.0 nm in order to monitor instrument drift. The determined analytical uncertainty was approximately  $\pm 2\text{--}4\%$  for the metals used in this study. The wavelengths used for the Cd, Zn and Pb analyses were 226.5, 206.2 and 220.4 nm, respectively.

#### 2.5. Surface complexation modeling

The deprotonation reaction of the proton-active thiol sites on the thiol-based resin beads can be described and modeled using the following reaction:

$$> R - SH^{\circ} \leftrightarrow > R - S^{-} + H^{+} \tag{2}$$

where >R denotes the macromolecule on the resins to which each thiol site is attached. The acidity constant of the thiol sites on the resins,  $K_a$ , can be expressed as:

$$K_a = \frac{\left[ \right\rangle R - S^- \right] a_{H^+}}{\left[ \right\rangle R - SH^0 \right]} \tag{3}$$

where  $[\normalfont{}\normalfo$ 

The calculated  $pK_a$  value and the calculated concentration of protonactive thiol sites on the BT40 resin were then used to model the metal adsorption data. We attempted to model the adsorption data using 1:2 and 1:1 metal:thiol stoichiometric ratios that were reported in previous studies of metal-thiol complexation [11,31], and we found that a 1:2 metal:thiol ratio failed to fit the adsorption data. Therefore, metal adsorption onto the BT40 resin was described using the following reaction:

$$>R-S^-+M^{2+}\leftrightarrow>R-S-M^+ \tag{4}$$

where  $>R-S^-$  represents the deprotonated form of thiol sites on the BT40 resin bead surface and  $>R-S-M^+$  represents the surface complex formed on the resin between a thiol site and a metal cation. The thermodynamic stability constant of the  $>R-S-M^+$  surface complex, K, can be expressed as:

$$K = \frac{[R - S - M^{+}]}{[R - S^{-}] \quad a_{M^{2+}}}$$
 (5)

where  $a_{M^{2+}}$  is the activity of  $M^{2+}$  in bulk solution, and the brackets represent the concentrations of the species shown. FITEQL 2.0 [29] was used as a modeling tool for optimization of the stability constants (K) of the metal-thiol surface complexes. For both the potentiometric titration modeling and the modeling of the metal adsorption measurements, a non-electrostatic surface complexation model (NEM) was used. Although ionic strength effects on both the proton and metal adsorption behavior are possible, we measured adsorption only under one ionic strength condition and hence our data cannot constrain electric field model parameters. Potentiometric titration and metal adsorption

experiments need to be conducted as a function of ionic strength in order to determine which surface electric field model can best account for the observed effects of ionic strength on the surface electric field of the resin beads.

#### 3. Results

Potentiometric titration results show that the three resins have significantly different buffering capacities (Fig. 1a), and surprisingly the buffering capacity is not correlated to the total concentration of thiol sites on the resins as reported by the bead manufacturers. The manufacturers of the SP70 and SP300 resins report that the beads contain at least 2.4 mmol/g of thiol sites, but the titration curves of the two resins are not significantly different from the titration curve of the thiol-free 0.01 M NaCl blank solution. This result suggests that if the SP70 and the SP300 resin beads contain thiol sites as reported by the manufacturer, then very few of the thiol sites on either of these resins are available for reaction with the added acid or base during the titrations. We attempted to model the SP70 and the SP300 titration data using our surface complexation modeling approach but were unsuccessful, likely due to the extremely low buffering capacity of these two resins. In contrast, the BT40 resin, with a manufacturer-reported thiol concentration of only 1.3 mmol/g, exhibited a much stronger buffering capacity than the other two resins. The BT40 resin, like the other two resins, exhibits no buffering capacity below a pH of approximately 8, but has a strong buffering response above pH 8 with the 'Net H<sup>+</sup> added' increasing from approximately 0 mmol/L at pH 8 to -4 mmol/L at pH 10. A one-site SCM fits the BT40 resin potentiometric titration data well (Fig. 1b), with a calculated average site concentration of 0.60  $\pm$  0.09 mmol/g and a calculated p $K_a$  of 10.2  $\pm$  0.1 for the triplicate titrations of the BT40 resin.

In general, the Cd adsorption kinetics measurements (Fig. 2) are consistent with the potentiometric titration results reported above. After 1 h of reaction time, the concentration of Cd remaining in solution in the BT40 resin experiments was below the detection limit of the ICP-OES measurement, but the SP70 and SP300 resins only removed approximately 20% and 5% of the aqueous Cd, respectively. Extending the reaction time from 1 h to 24 h did not increase the amount of Cd removed by the BT40 or SP70 resins, suggesting that the adsorption of Cd onto the BT40 and SP70 resins reaches equilibrium in the first 1 h. For the SP300 resin, increasing the reaction time increased the concentration of Cd removed to some extent, likely due to the bigger size of the SP300 resin beads than the other two resins. For porous materials like resins and activated carbon, intra-particle diffusion typically controls the adsorption kinetics [32-34] and hence it takes longer for the aqueous Cd to be transported to the thiol sites within the pores of larger resin particles like the SP300 resin. However, the extent of Cd adsorption onto the SP300 resin beads increased only moderately, from approximately 5-9%, even after 24 h of reaction. Because the BT40 resin beads exhibit the greatest

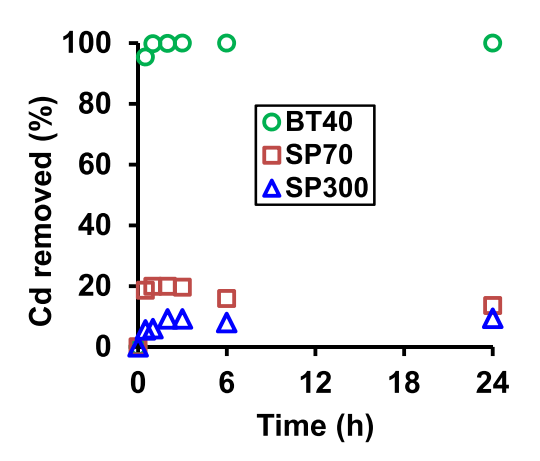
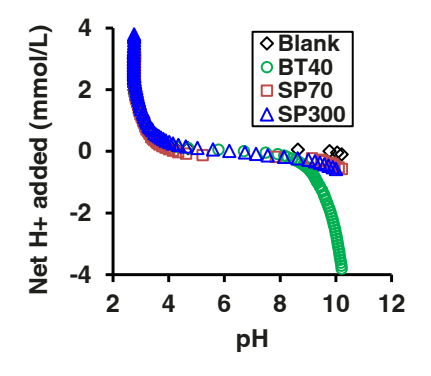


Fig. 2. Kinetics of Cd adsorption onto the BT40, SP70 and SP300 resin beads. The experiments were conducted with  $10\ mg/L$  of Cd and  $10\ g/L$  of resin in 0.01 M NaCl solutions at pH 6.

extent of Cd adsorption, we chose to use it in our subsequent adsorption experiments whose objective was to compare the adsorption behaviors of different chalcophile metals and to use the results to develop a predictive model of metal adsorption onto resin beads.

In order to test if the SCM approach can be used to predict the adsorption behavior of chalcophile metals onto the BT40 resin, we first measured the adsorption of Cd onto the BT40 resin as a function of pH and metal:resin ratio. The pH adsorption edges at different Cd:resin ratios follow similar trends (Fig. 3). The extent of Cd adsorption increases with increasing solution pH from pH 3-5 or 6, and reaches a plateau at higher pH values. Given that the thiol site has a  $pK_a$  value of  $10.2 \pm 0.1$  and that we measured significant adsorption well below pH 10.2, the observed adsorption edges suggest that strong, and likely covalent, bonding between Cd and the surface thiol sites occurs [31,35,36] and is responsible for the Cd adsorption behavior. Note also that the measured concentration of thiol sites on the BT40 resin is 0.60  $\pm$  0.09 mmol/g, a value which is greater than the total Cd concentration in the 0.22 and the 0.45 mmol/g experiments. Under these conditions, the observed adsorption plateaus occur because of Cd limitation, and all of the aqueous Cd is adsorbed onto the resin above pH 5-6. However, in the 0.89 mmol/g Cd:resin ratio experiments, the maximum extent of Cd adsorption onto the resin that we measured is 0.63 mmol/g at pH 7.2. This result suggests that under a Cd:resin ratio of 0.89 mmol/g, the experiments are site limited, and the plateau that we observed in the extent of Cd adsorption is due to the saturation of thiol sites on the resin. These experiments not only strongly suggest that the Cd-thiol surface complex exhibits a 1:1 Cd:thiol molal stoichiometry, but also that all of the thiol sites on the BT40 resin beads are accessible for Cd adsorption on the timescale of these experiments.

We attempted to fit the Cd adsorption data using a one-site surface



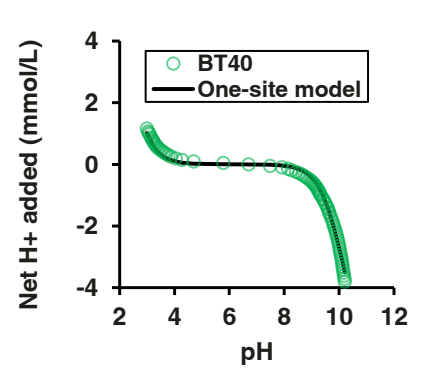
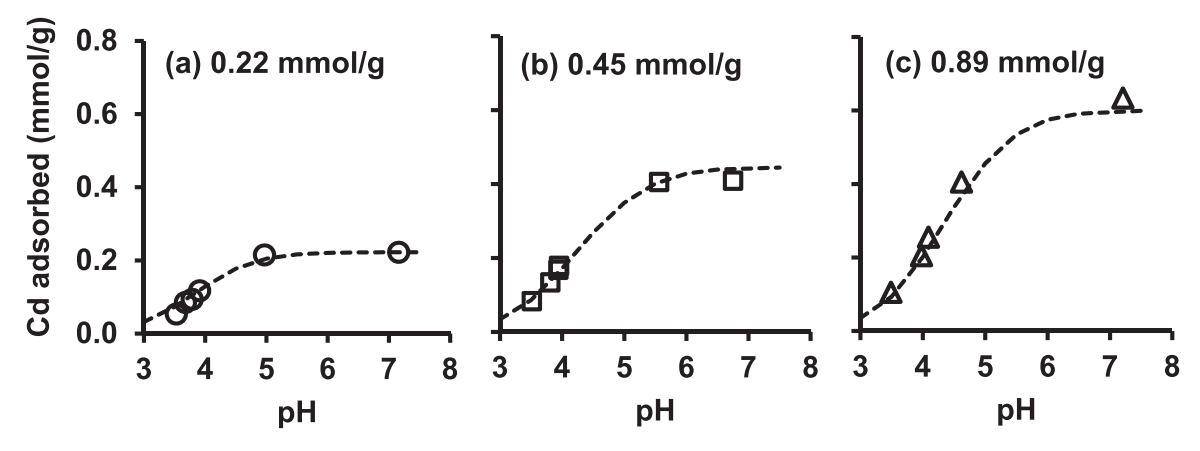


Fig. 1. (a) Potentiometric titration curves for 0.01 M NaCl solutions containing either no resin (blank) or 10 g/L of BT40, SP70 or SP300 resins; (b) Fitting curve for a representative titration of the BT40 resin by a non-electrostatic one-site surface complexation model.



**Fig. 3.** Cd adsorption onto the BT40 resin at different Cd:resin ratios: (a) 0.22 mmol/g; (b) 0.45 mmol/g; (c) 0.89 mmol/g. Dashed curves represent one-site surface complexation modeling predictions using a log *K* value for the surface complexation reaction (Reaction 4) of 9.72, the average of the calculated log *K* values from the three Cd:resin ratio conditions studied.

complexation model based on a 1:1 Cd:thiol stoichiometry for the Cd surface complex, and found that the model provides an excellent fit to the data both as a function of pH and as a function of Cd:resin ratio. We modeled each set of experiments with fixed Cd:resin ratios separately, and the calculated log K (stability constant) values for the Cd-thiol surface complex (Reaction 4) on the resin are 9.61, 9.74 and 9.81 for the Cd:resin ratios of 0.22, 0.45 and 0.89 mmol/g, respectively, with an average log K value of 9.72  $\pm$  0.10 (1 $\sigma$ ). We used this average K value to predict the extent of Cd adsorption onto the resin that would occur under the different conditions, and we found that the predicted extents of adsorption (dashed curves in Fig. 3) are in excellent agreement with the measured extents of adsorption. This result suggests that a single K value can account for the Cd adsorption behavior onto the BT40 resin beads both as a function of pH and Cd:resin ratio, and that the SCM approach can be used to predict Cd adsorption behavior under conditions not directly studied in the laboratory.

In order to determine relationships between the adsorption behaviors of different chalcophile elements, we also measured the adsorption of Zn onto the BT40 resin using the same approach. The extent of Zn adsorption is negligible at and below approximately pH 4, and increases with increasing solution pH above pH 4 (Fig. 4). The measured extent of Zn adsorption is less than the extent of Cd adsorption that we measured under similar conditions. For example, the extent of Zn adsorption onto the BT40 resin is negligible at pH 3–4 at each of the three Zn:resin ratios studied, while the extent of Cd adsorption is approximately 0.1 mmol/g at pH 3–4 even under the lowest Cd:resin ratio of 0.22 mmol/g.

Although the resin contains a thiol site concentration of 0.60  $\pm$  0.09 mmol/g, approximately 36% of the total Zn in these experiments remained in solution even at a pH of 6.87 in the experiments with a Zn loading of 0.45 mmol/g. The extent of Cd adsorption under these metal: resin ratio and pH conditions was limited by the total concentration of Cd in the system, and hence these experiments demonstrate that the affinity of the surface thiol sites for Zn is markedly less than that for Cd. As was the case for the Cd adsorption data, a one-site NEM surface complexation model with a 1:1 Zn:thiol surface complex stoichiometry vields an excellent fit to the Zn adsorption data (Fig. 4). As we did with the Cd data, we modeled each set of Zn adsorption data with a fixed Zn: resin ratio separately, and the calculated log K values for the Zn-thiol surface complex on the resin are 7.68, 7.47 and 7.58 for the Zn:resin ratios of 0.23, 0.45 and 0.91 mmol/g, respectively, with an average of  $7.58 \pm 0.11$  (1 $\sigma$ ). Note that although this K value is significantly below that calculated for the Cd-thiol surface complex, it still suggests strong and likely covalent bonding between the Zn and the surface thiol sites [37–39]. As is the case for Cd, extensive Zn adsorption was observed at pH values well below 10.2, the  $pK_a$  value of the surface thiol sites. We used the average log K value of 7.58 to predict the extent of Zn adsorption onto the BT40 resin as a function of pH under the three Zn: resin ratios studied. These predictions (dashed curves in Fig. 4) are in excellent agreement with the measured Zn adsorption data both as a function of Zn:resin ratio and pH, again demonstrating the ability of the SCM approach to account for the effects of a range of system parameters on Zn adsorption onto the BT40 resin.

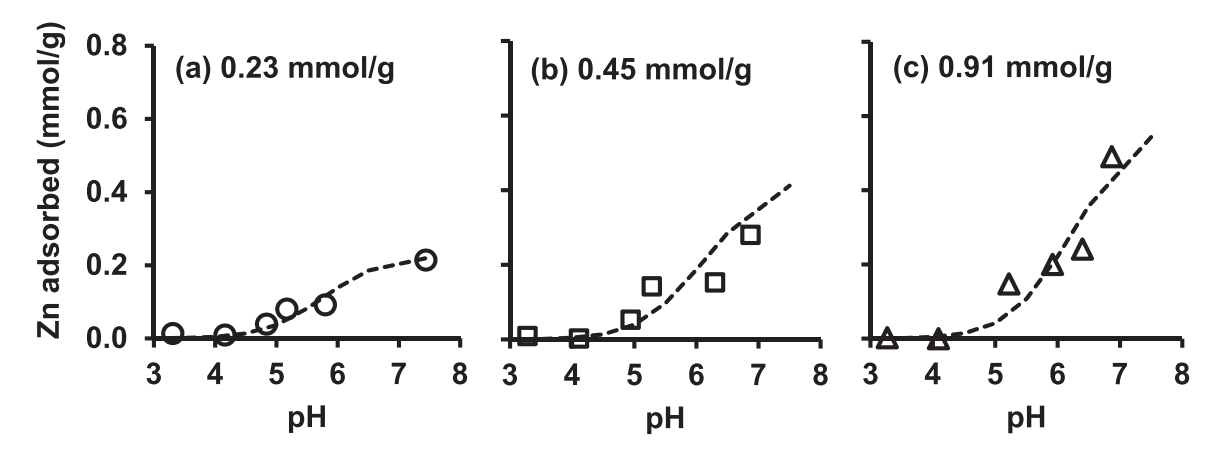


**Fig. 4.** Zn sorption onto the BT40 resin at different Zn:resin ratios: (a) 0.23 mmol/g; (b) 0.45 mmol/g; (c) 0.91 mmol/g. Dashed curves represent one-site surface complexation modeling predictions using a log *K* value for the surface complexation reaction of 7.58, the average of the calculated log *K* values from the three Zn: resin ratio conditions studied.

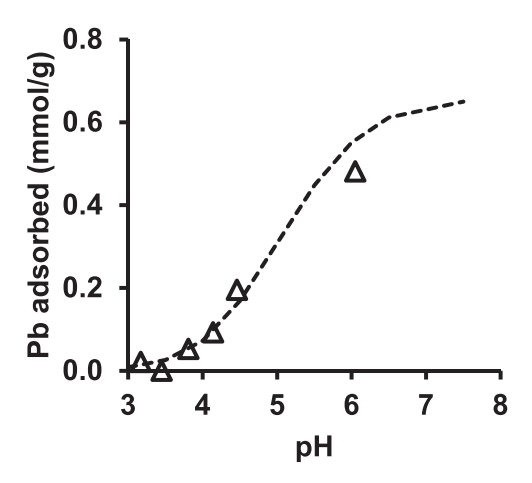


**Fig. 5.** Pb adsorption onto the BT40 resin at a Pb:resin ratio of 0.90 mmol/g. The dashed curve represents the best-fitting one-site non-electrostatic surface complexation model of the data with a log *K* value for the surface complexation reaction of 9.19.

In addition to Cd and Zn adsorption, we also measured the adsorption of Pb onto the BT40 resin as a function of pH at a Pb:resin ratio of 0.90 mmol/g (Fig. 5). The measured extent of Pb adsorption is greater than that of Zn adsorption at a given pH and under similar metal:resin ratio conditions, but is less than that of Cd adsorption. As was the case in modeling the Zn and Cd adsorption data, a one-site surface complexation model with a 1:1 Pb-thiol surface complex stoichiometry provides a good fit to the data, and the calculated log K value for the Pb-thiol surface complex is  $9.19 \pm 0.09$  (1 $\sigma$ ). Because only one Pb:resin ratio condition was studied in the Pb system, the uncertainty associated with the calculated K value was determined by using FITEQL2.0 to calculate the Pb adsorption behavior with a fixed K value for the Pb adsorption reaction. By varying the K value manually, we determined the range of K values that encompassed all the data. The determined K range represents  $3\sigma$  from the average K value, and was used to calculate the reported  $1\sigma$ uncertainty of the K value of Pb-thiol surface complex.

Applying the SCM approach to predict metal adsorption onto thiol-based resin surfaces requires that the stability constant for each important surface complexation reaction (e.g., Reaction 4) be determined. One method that has been used to estimate K values for a wide range of metals of interest in the absence of experimental data has been to use linear free-energy relationships (LFERs) [40,41], which in the case of thiol-based resins relate measured K values of metal-thiol surface

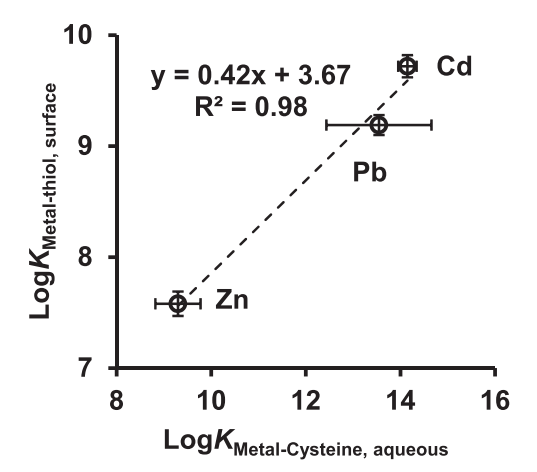


**Fig. 6.** Linear free energy relationship (LFER) between the calculated Log K values for the metal-thiol surface complexes on the BT40 resin measured in this study and the corresponding Log K values for metal-cysteine aqueous complexes. The dashed line represents the linear fit to the data.

complexes involving the resin of interest to known K values of metal-thiol aqueous complexes. In order to determine a LFER for the BT40 resin, we related the log K values of the Cd-, Zn-, and Pb-thiol surface complexes that we measured for the BT40 resin to the log K values of the corresponding metal-cysteine aqueous complexes for those same metals [42]. The results are depicted in Fig. 6, which illustrates a strong linear correlation between the two types of K values, with a  $\mathbb{R}^2$  of 0.983. This result suggests that metal cations interact similarly to thiol binding sites whether the sites are on an aqueous molecule such as cysteine or on a thiol-treated surface such as the BT40 resin. The linearity of the relationship suggests that the LFER can be applied to estimate the K values of metal-thiol surface complexes on the BT40 resin for other chalcophile metals that were not studied here, based solely on known K values of the corresponding metal-cysteine aqueous complexation reaction. The linear relationship shown in Fig. 6 is:

$$Log K_{metal-thiol, surface} = 0.42*Log K_{metal-cysteine, aqueous} + 3.67$$
 (6)

# 4. Discussion

One important finding of this study is that the proton and metal adsorption capacities of thiol-based resins are not related to the manufacturer's reported total concentration of thiol sites on the resins. As shown in Fig. 2, although the SP300 resin is reported to contain 4.8-5.0 mmol/g of total thiol sites on its surface, the resin removed no more than 10% of the total Cd from solution after 1 h, despite the experimental system having a theoretical excess of thiol sites relative to Cd in solution (the reported molal concentration of surface thiol sites was approximately 22 times greater than the total molal Cd concentration in the experiment). In contrast, the BT40 resin, which is reported to contain only 1.3 mmol/g of total thiol surface sites, removed 100% of the Cd from solution after 1 h. Clearly, the BT40 resin actually has a higher concentration of Cd-accessible thiol sites than the SP300 resin. Silica-based resins have functional groups primarily on their surface, which are designed to improve the poor mass transfer kinetics of polystyrene resins that have functional groups throughout the threedimensional volume of the whole resin bead [43]. Therefore, it is possible that it takes longer for aqueous Cd cations to diffuse into a polystyrene resin like SP300 and to reach the thiol sites. However, neither extending the reaction time to 24 h for the SP300 resin nor replacing the SP300 resins with SP70, a smaller version of SP300, made more thiol sites accessible and the extent of Cd adsorption remained low for both resin types (Fig. 2). It is more likely that either the manufacturer's reported thiol concentrations are inaccurate, or that the type of thiol sites on thiol-based resins can strongly affect the extent of Cd and proton adsorption onto the resins. Compared with the thiolphenol, which is present on the SP300 and SP70 resin beads, the propanethiol molecules on the BT40 resin are more flexible and would lead to fewer steric hindrances for the binding of Cd cations on the surface, so this difference may contribute to the higher extent of Cd adsorption onto the BT40 resin compared to the other two resin types.

Because only a portion of the manufacturer's reported concentration of thiol sites on thiol-based resins are available for proton and metal binding, it is crucial to quantify the concentration and binding affinity of this portion of thiol sites on the resins, and we refer to them in the following text as 'effective thiol sites' to differentiate from the manufacturer's reported concentrations of thiol sites. Our results suggest that measuring the concentration of proton-active sites through the use of potentiometric titrations combined with surface complexation modeling provides a means for quantifying the effective thiol site concentration on a resin material of interest (Figs. 1 and 2). A proton-active thiol site is a site that can react easily and rapidly with H<sup>+</sup>/OH<sup>-</sup>. Because protons are smaller than any metal cations, the thiol sites that are inaccessible to protons will most likely also be inaccessible to metal cations as well. As

our results show, the calculated  $pK_a$  of the thiol sites on the BT40 resin is  $10.2\pm0.1$ , which indicates that virtually all of the thiol sites are in their protonated uncharged form under the pH ranges we studied. Therefore, the adsorption of metal cations onto these thiol sites on the BT40 resin involves the replacement of the proton that is bound to a thiol site by a metal cation, and can only occur on those proton-active thiol sites that are accessible to aqueous metal cations. In other words, if a thiol site does not respond to the changes in pH that occur during a potentiometric titration experiment, then it would be unlikely to be able to bind metal cations. This explanation accounts for why the SP300 and SP70 resins, which have very few proton-active sites, also exhibit a low adsorption capacity for Cd. Conversely, the BT40 resin, which our experiments show contains  $0.60 \pm 0.09 \text{ mmol/g}$  of proton-active thiol sites, could adsorb up to 0.63 mmol/g of Cd in the presence of an excess of Cd (0.89 mmol of Cd per gram of resin). These results suggest that the proton-active sulfhydryl sites represent the effective thiol sites which are active in the adsorption of chalcophile metals, and that their concentration, as determined by potentiometric titrations, is a good indicator for metal adsorption capacity of a thiol-based resin.

Once the concentration and  $pK_a$  value of the effective thiol sites are determined for a resin of interest, it is possible to use metal adsorption measurements to calculate the stability constant (K) of the formed metal-thiol surface complexes on thiol-based resins. In this study, the calculated K values for metal-thiol complexes on the BT40 resin do not vary systematically or significantly as a function of metal:resin ratios for either Cd or Zn, suggesting that the metal-thiol surface complexation reactions can be quantified using the principles of chemical equilibrium thermodynamics, similar to the surface complexation reactions involving other materials [22,44]. These results also suggest that the concentration of effective thiol sites on the resin does not change as a function of metal:resin ratio. Otherwise, the calculated K values would change due to the change in the concentration of effective thiol sites. As shown in Figs. 3 and 4, the surface complexation model, using the measured effective thiol site concentration and the average value of the calculated metal-thiol stability constant, K, accounts for both pH and metal:resin ratio effects on the adsorption of Zn and Cd onto the BT40 resin. These results strongly suggest that these surface complex stability constants and this modeling approach can also predict the adsorption of Zn and Cd under a wide range of other conditions as well. For example, the same set of equilibrium constants and site concentrations can be used to estimate the effects of the presence of ligands such as chloride and organic acid anions on the Zn and Cd adsorption behavior. Because the log K values of the metal-thiol surface complexes on the resin are strongly linearly correlated to the log K values of their corresponding metal-cysteine aqueous complexes (Fig. 6), and because the K values of aqueous metal-cysteine complexes are available for most chalcophile metals, we can use Eq. (6) to estimate the K value for surface complexes formed between the thiol sites on the resin and other metals whose adsorption onto the resin has not been measured. Therefore, the results of this study can be used to predict the extent of adsorption of a wide range of metals onto thiol-based resins under a wide range of system conditions. It should be noted that Eq. (6) can only estimate the *K* value for a 1:1 metal:thiol surface complex on the BT40 resin. For metals, such as Hg [45,46], that form multiple types of surface complexes with thiols on a single thiol-bearing surface, it is important to measure metal adsorption onto thiol resins over a wide range of metal:resin ratios in order to constrain a K value for each of the metal-thiol surface complexes that form.

## 5. Conclusions

This study demonstrates that surface complexation modeling is a powerful tool for determining the adsorption capacity of thiol-coated resins for chalcophile metals. The accurate measurement of the effective thiol site concentration on thiol-coated resins through the use of potentiometric titrations and surface complexation modeling can help

rapidly select the best resin and the best operating conditions for the separation of chalcophile metals from solution. The stability constant for a metal-thiol surface complex, obtained by modeling metal adsorption data, can be used to predict not only the adsorption of this metal onto the resin as a function of pH and metal:resin ratio, but also the adsorption of other chalcophile metals that have not been studied experimentally onto the resin. Together, these approaches can aid in the design and optimization of strategies for the separation and recovery of chalcophile metals from various aqueous media, making the use of precious metals more sustainable and diminishing the discharge of toxic metals to the environment.

# CRediT authorship contribution statement

**Qiang Yu:** Conceptualization, Methodology, Investigation, Visualization, Writing – original draft. **Jeremy B. Fein:** Conceptualization, Project administration, Funding acquisition, Writing – review & editing.

#### **Declaration of Competing Interest**

The authors declare the following financial interests/personal relationships which may be considered as potential competing interests: Jeremy Fein reports financial support was provided by National Science Foundation.

#### Data availability

Data will be made available on request.

### Acknowledgments

QY was supported through the Center for Environmental Science and Technology at University of Notre Dame. The research was funded in part by U.S. National Science Foundation grants EAR-1904192 and EAR-2149717.

### References

- [1] L. Jarup, Hazards of heavy metal contamination, Br. Med. Bull. 68 (2003) 167-182.
- [2] L. Canda, T. Heput, E. Ardelean, Methods for recovering precious metals from industrial waste, IOP Conf. Ser. Mater. Sci. Eng. 106 (1) (2016) 012020.
- [3] B. Volesky, Z.R. Holan, Biosorption of heavy-metals, Biotechnol. Prog. 11 (3) (1995) 235–250.
- [4] S.E. Bailey, et al., A review of potentially low-cost sorbents for heavy metals, Water Res. 33 (11) (1999) 2469–2479.
- [5] T.A. Kurniawan, et al., Physico-chemical treatment techniques for wastewater laden with heavy metals, Chem. Eng. J. 118 (1–2) (2006) 83–98.
- [6] A. Taghvaie Nakhjiri, et al., Recovery of precious metals from industrial wastewater towards resource recovery and environmental sustainability: a critical review, Desalination 527 (2022), 115510.
- [7] X. Feng, et al., Functionalized monolayers on ordered mesoporous supports, Science 276 (5314) (1997) 923–926.
- [8] N. Huang, et al., Stable covalent organic frameworks for exceptional mercury removal from aqueous solutions, J. Am. Chem. Soc. 139 (6) (2017) 2428–2434.
- [9] Y.S. Shin, et al., Sulfur-functionalized mesoporous carbon, Adv. Funct. Mater. 17 (15) (2007) 2897–2901.
- [10] M. Nishizawa, et al., Preparation and metal-adsorption properties of polystyrene resins functionalized with multidentate ligands having nitrogen and sulfur donor sets. Polyhedron 5 (12) (1986) 2047–2049.
- [11] B. Saha, et al., Sorption of trace heavy metals by thiol containing chelating resins, Solvent Extr. Ion Exch. 18 (1) (2000) 133–167.
- [12] A. Khojastehnezhad, et al., Postsynthetic modification of core-shell magnetic covalent organic frameworks for the selective removal of mercury, ACS Appl. Mater. Interfaces 15 (23) (2023) 28476–28490.
- [13] X. Liang, et al., Preparation, characterization of thiol-functionalized silica and application for sorption of Pb2+ and Cd2+, Colloids Surf. A Physicochem. Eng. Asp. 349 (1) (2009) 61–68.
- [14] H.Y. Choi, et al., Thiol-functionalized cellulose nanofiber membranes for the effective adsorption of heavy metal ions in water, Carbohydr. Polym. 234 (2020), 115881
- [15] C.M. Bethke, P.V. Brady, How the Kd approach undermines ground water cleanup, Groundwater 38 (3) (2000) 435–443.
- [16] C.M. Koretsky, Predicting Adsorption in Natural Systems: Are We There Yet? (Invited), 2010, p. B43G-01.

- [17] K. Leus, et al., UiO-66-(SH)2 as stable, selective and regenerable adsorbent for the removal of mercury from water under environmentally-relevant conditions, Faraday Discuss. 201 (0) (2017) 145–161.
- [18] J.A. Davis, D.B. Kent, Chapter 5. Surface complexation modeling in aqueous geochemistry, in: F.H. Michael, F.W. Art (Eds.), Mineral-Water Interface Geochemistry, De Gruyter, Berlin, Boston, 1990.
- [19] J.B. Fein, et al., A chemical equilibrium model for metal adsorption onto bacterial surfaces, Geochim. Cosmochim. Acta 61 (16) (1997) 3319–3328.
- [20] T.D. Waite, et al., Uranium(VI) adsorption to ferrihydrite: application of a surface complexation model, Geochim. Cosmochim. Acta 58 (24) (1994) 5465–5478.
- [21] H. Ching-kuo Daniel, D. Langmuir, Adsorption of uranyl onto ferric oxyhydroxides: application of the surface complexation site-binding model, Geochim. Cosmochim. Acta 49 (9) (1985) 1931–1941.
- [22] C. Chen, et al., Surface complexation modeling of Sr(II) and Eu(III) adsorption onto oxidized multiwall carbon nanotubes, J. Colloid Interface Sci. 323 (1) (2008) 33-41
- [23] C.R. Evanko, D.A. Dzombak, Surface complexation modeling of organic acid sorption to goethite, J. Colloid Interface Sci. 214 (2) (1999) 189–206.
- [24] Y. Zhang, X. Tang, W. Luo, Metal removal with two biochars made from municipal organic waste: adsorptive characterization and surface complexation modeling, Toxicol. Environ. Chem. 96 (10) (2014) 1463–1475.
- [25] J. Han, S.M. Nomaan, L.E. Katz, Prediction of alkaline earth metal ion adsorption on goethite for various background electrolytes with the CD-MUSIC model, Sci. Total Environ. 892 (2023), 164462.
- [26] A.M.S. Oancea, et al., Langmuir and surface complexation models for ion exchange equilibria on strong acid resins, J. Ion Exch. 18 (4) (2007) 162–167.
- [27] Z. Xu, et al., Co-adsorption and interaction mechanism of cadmium and sulfamethazine onto activated carbon surface, Colloids Surf. A Physicochem. Eng. Asp. 619 (2021), 126540.
- [28] A.K. Mosai, R.H. Johnson, H. Tutu, Modelling of palladium(II) adsorption onto amine-functionalised zeolite using a generalised surface complexation approach, J. Environ. Manag. 277 (2021), 111416.
- [29] J.C. Westall, FITEQL, A Computer Program for Determination of Chemical Equilibrium Constants from Experimental Data, Version 2.0. Report 82-02. 1982, Department of Chemistry, Oregon State University, Corvallis, OR, USA.
- [30] J.B. Fein, et al., Potentiometric titrations of Bacillus subtilis cells to low pH and a comparison of modeling approaches, Geochim. Cosmochim. Acta 69 (5) (2005) 1123–1132.

- [31] B. Mishra, et al., High- and low-affinity binding sites for Cd on the bacterial cell walls of Bacillus subtilis and Shewanella oneidensis, Geochim. Cosmochim. Acta 74 (15) (2010) 4219–4233.
- [32] S. Rengaraj, et al., Kinetics of removal of chromium from water and electronic process wastewater by ion exchange resins: 1200H, 1500H and IRN97H, J. Hazard. Mater. 102 (2) (2003) 257–275.
- [33] R. Leyva-Ramos, et al., Intraparticle diffusion of cadmium and zinc ions during adsorption from aqueous solution on activated carbon, J. Chem. Technol. Biotechnol. 80 (8) (2005) 924–933.
- [34] F. Liu, et al., Adsorptive recovery of Au(III) from aqueous solution using crosslinked polyethyleneimine resins, Chemosphere 241 (2020), 125122.
- [35] D. Chen, et al., The mechanism of cadmium sorption by sulphur-modified wheat straw biochar and its application cadmium-contaminated soil, Sci. Total Environ. 714 (2020), 136550.
- [36] T. Karlsson, et al., Complexation of cadmium to sulfur and oxygen functional groups in an organic soil, Geochim. Cosmochim. Acta 71 (3) (2007) 604–614.
- [37] C. Hübner, H. Haase, Interactions of zinc- and redox-signaling pathways, Redox Biol. 41 (2021), 101916.
- [38] S. Wei, et al., Monolayer thiol engineered covalent interface toward stable zinc metal anode, ACS Nano 16 (12) (2022) 21152–21162.
- [39] B.P. Kennedy, A.B.P. Lever, Studies of the metal-sulfur bond. Complexes of the pyridine thiols, Can. J. Chem. 50 (21) (1972) 3488–3507.
- [40] J.B. Fein, A.M. Martin, P.G. Wightman, Metal adsorption onto bacterial surfaces: development of a predictive approach, Geochim. Cosmochim. Acta 65 (23) (2001) 4267 4272
- [41] R.M. Nell, J.B. Fein, Influence of sulfhydryl sites on metal binding by bacteria, Geochim. Cosmochim. Acta 199 (2017) 210–221.
- [42] R.M. Smith, A.E. Martell, Critical Stability Constants, Plenum Press, New York, 1976.
- [43] J.L. Wood, The Structure Function Relationship of Silica Polyamine Composites, The University of Montana, 2008.
- [44] Q. Yu, J.B. Fein, The effect of metal loading on Cd adsorption onto Shewanella oneidensis bacterial cell envelopes: the role of sulfhydryl sites, Geochim. Cosmochim. Acta 167 (2015) 1–10.
- [45] B. Mishra, et al., Stoichiometry of mercury-thiol complexes on bacterial cell envelopes, Chem. Geol. 464 (2017) 137–146.
- [46] Y. Song, et al., Toward an internally consistent model for Hg(II) chemical speciation calculations in bacterium–natural organic matter–low molecular mass thiol systems, Environ. Sci. Technol. 54 (13) (2020) 8094–8103.